Proc. Natl. Acad. Sci. USA
Vol. 89, pp. 9895–9899, October 1992
Biophysics

A single-pool inositol 1,4,5-trisphosphate-receptor-based model for agonist-stimulated oscillations in Ca^{2+} concentration

GARY W. DE YOUNG† AND JOEL KEIZER

Institute of Theoretical Dynamics and Department of Chemistry, University of California, Davis, CA 95616

Communicated by Terrell L. Hill, May 18, 1992 (received for review March 19, 1992)

ABSTRACT **Relying on quantitative measurements of Ca^{2+} activation and inhibition of the inositol 1,4,5-trisphosphate (IP_3) receptor in the endoplasmic reticulum, we construct a simplified kinetic model to describe the properties of this channel. Selecting rate constants to fit key kinetic and equilibrium data, we find that the model reproduces a variety of *in vivo* and *in vitro* experiments. In combination with Ca^{2+}-ATPase activity for Ca^{2+} uptake into the endoplasmic reticulum, the model leads to cytoplasmic oscillations in Ca^{2+} concentration at fixed IP_3 concentration and only a single pool of releasable Ca^{2+}, the endoplasmic reticulum. Incorporation of a positive-feedback mechanism of Ca^{2+} on IP_3 production by phospholipase C enriches the properties of the oscillations and leads to oscillations in Ca^{2+} concentration accompanied by oscillations in IP_3 concentration. We discuss the possible significance of these results for the interpretation of experiments.**

Several mechanisms have been proposed to explain oscillations of intracellular Ca^{2+} concentration in nonexcitable cells (see refs. 1 and 2 for reviews). Generally speaking, the models fall into three broad categories: (*i*) Ca^{2+}-initiated Ca^{2+} release (3), (*ii*) agonist-receptor oscillations mediated by G proteins, diacylglycerol, and protein kinase C (4), and (*iii*) positive feedback of Ca^{2+} on the production of inositol 1,4,5-trisphosphate (IP_3) through membrane-bound phospholipase C (PLC) (2, 5). Depending on cell type (6, 7), it is possible that some fluctuation in IP_3 concentration might occur.

Here we examine the recent proposal (8–10) that a biphasic response of the IP_3 receptor/channel to cytosolic Ca^{2+} might be sufficient to induce Ca^{2+} oscillations. Indeed, Finch *et al.* (8) have shown that the IP_3-induced efflux of Ca^{2+} from microsomal vesicles was first enhanced, and then inhibited, as extravesicular Ca^{2+} was increased from 100 nM to 100 μM. In Purkinje cells of the cerebellum, Ca^{2+} is required for the IP_3 receptor/channel to open (9). At Ca^{2+} basal concentrations well below $\approx$0.25 μM, increasing $[Ca^{2+}]$ increases the open probability of the IP_3 receptor/channel. For $[Ca^{2+}]$ higher than 0.25 μM, however, the open probability decreases. Joseph *et al.* (11) observed a similar biphasic effect in their study of Ca^{2+} release from cerebellum microsomal fractions (figure 4 of ref. 11). The experiments of Parker and Ivorra (12) also showed that small releases of Ca^{2+} from the IP_3-sensitive store in *Xenopus* oocytes facilitate a second release, while larger Ca^{2+} releases have an inhibitory effect.

We present here a simplified model of the kinetics of the IP_3 receptor/channel that is based on the open probability data of Bezprozvanny *et al.* (9) and the IP_3 binding data of Joseph *et al.* (11). From this model we are able to predict both the biphasic dependence of the open probabilities on $[Ca^{2+}]$ and its maximal value as a function of $[IP_3]$. We also find it to be consistent with the single- and double-pulse IP_3 experiments in *Xenopus* (12). When combined with a Ca^{2+} uptake step into the endoplasmic reticulum (ER), the model of the IP_3 receptor/channel produces $[Ca^{2+}]$ oscillations for constant $[IP_3]$. The model also supports oscillations when Ca^{2+} is allowed to feedback upon the production rate of IP_3 through PLC, leading to in-phase oscillations in $[IP_3]$ (5).

IP_3 Receptor/Channel

The IP_3 receptor/Ca^{2+} channel is thought to be composed of four identical subunits (13, 14). Watras *et al.* (15) found in bilayer voltage clamp experiments that the IP_3 receptor/channel opens to four distinct conductance levels, each corresponding to a 20-pS increase in the conductance. The channel, however, most frequently opens to the third level (60 pS), which has an open time that is greater than the open times for the other conductance states (15). Under assumptions that ignored the different conductance levels, Bezprozvanny *et al.* (9) showed that the steady-state open probability is fit well by the functional form

$$\left[\frac{[Ca^{2+}]k}{([Ca^{2+}]+K)([Ca^{2+}]+k)}\right]^m,$$

where $K = k = 0.2$ μM and $m = 2.7$.

We construct a simplified model of the IP_3 receptor/channel by assuming that three equivalent and independent subunits are involved in conduction. While it is probable that the subunits are in fact not independent of one another, improvements in this aspect of the model need to await more detailed kinetic measurements. We further assume that each subunit has one IP_3 binding site and two Ca^{2+} binding sites, one for activation, the other for inhibition. Thus, each subunit may exist in eight states with transitions governed by second-order (a_i) and first-order (b_i) rate constants (Fig. 1). We label the binding sites as 1, 2, and 3, and introduce the notation $S_{i_1i_2i_3}$, where i_j equals 0 or 1. The jth binding site is occupied if $i_j = 1$. Binding site 1 is the IP_3 binding site, site 2 is the Ca^{2+} activation site, and site 3 is the Ca^{2+} inactivation site. The fraction of subunits in state $S_{i_1i_2i_3}$ is denoted by $x_{i_1i_2i_3}$.

Since detailed kinetic parameters are not yet available for the interaction of the subunits, we assume for the present that only the state S_{110} (one IP_3 and one activating Ca^{2+} bound) contributes to the conductance and that all three subunits must be in this state for the channel to be open. Thus the open probability is proportional to x_{110}^3. Assuming mass action kinetics, the equations describing the dynamics of a subunit are easily written down (cf. ref. 5). We have fit the equilibrium state of these equations to the IP_3 binding data of Joseph *et al.* (11) and to the equilibrium open probability data of Bezprozvanny *et al.* (9).

The data of Joseph *et al.* (11) indicate that the effective K_d for IP_3 binding to microsomal ER fractions is increased by Ca^{2+}, from approximately $K_{d1} = 145$ nM in the absence of

The publication costs of this article were defrayed in part by page charge payment. This article must therefore be hereby marked "*advertisement*" in accordance with 18 U.S.C. §1734 solely to indicate this fact.

Abbreviations: IP_3, inositol 1,4,5-trisphosphate; PLC, phospholipase C; ER, endoplasmic reticulum.

†Present address: Mathematics Department, Western State College of Colorado, Gunnison, CO 81231.

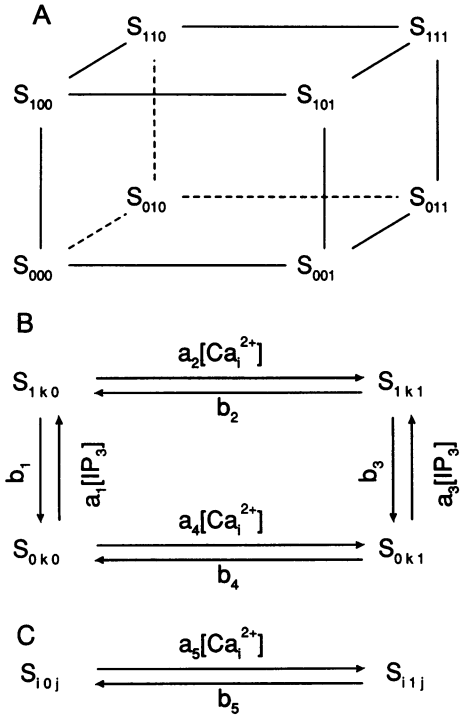

FIG. 1. A schematic diagram of the kinetics of an IP_3 receptor/channel subunit (see text for notation). (*A*) The eight possible states. (*B*) The kinetics on the front ($k = 0$) and back ($k = 1$) faces of the cube in *A*. (*C*) The kinetics of the Ca^{2+} activation binding site (transitions between the front and back faces of the cube in *A*).

calcium to $K_{d2} = 542$ nM in the presences of 1 μM Ca^{2+}. For simplicity we assume that Ca^{2+} directly affects the binding of IP_3. The equilibrium state for the receptor/channel subunits has been fit to the binding data of Joseph *et al.* (11), giving the equations (5):

$$d_1 = K_{d1} - \widehat{IP_3} \qquad [1a]$$

$$d_3 = (K_{d2} - \widehat{IP_3})(1 + d_2) - d_1 d_2, \qquad [1b]$$

where $d_i = b_i/a_i$ and $\widehat{IP_3} = 15$ nM is the concentration of labeled IP_3 used in the cold titration process at 0°C (11).

At equilibrium the open probability for an IP_3 receptor/channel is given by

$$P^e_{open} = (x^e_{110})^3 =$$

$$\left[\frac{[Ca^{2+}][IP_3]d_2}{([Ca^{2+}][IP_3] + [IP_3]d_2 + d_1 d_2 + [Ca^{2+}]d_3)([Ca^{2+}] + d_5)}\right]^3,$$

where x^e_{110} is the equilibrium fraction of subunits in state S_{110}. Given Eqs. 1, d_2 and d_5 were chosen so that P^e_{open} agrees with Bezprozvanny *et al.* (9), who found that for $[IP_3] = 2$ μM a maximum open probability of 0.15 occurred at $[Ca^{2+}] = 0.25$ μM. Finally, we use the thermodynamic constraint (16) to determine d_4 ($d_4 = d_1 d_2/d_3$). The values of d_i that are determined by these measurements are given in Table 1. Since the d_i values are uniquely determined, it is possible to calculate the maximum equilibrium open probability under a variety of conditions. Fig. 2*A* shows P^e_{open} as a function of $[Ca^{2+}]$ for $[IP_3] = 2$ μM. Fig. 2*B* shows P^e_{open} as a function of $[IP_3]$ for $[Ca^{2+}] = 0.1$ μM. Both curves are in good qualitative agreement with the experimental data, except that the sensitivity of the channel to IP_3 is decreased (Fig. 2*B*). Note that with the parameters in Table 1, the peak open probability shifts to the left with increasing IP_3, a feature that

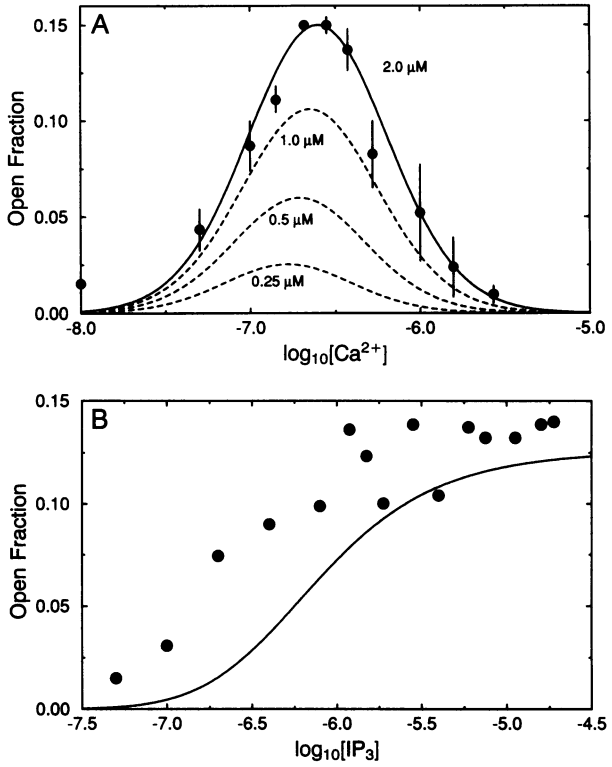

FIG. 2. (*A*) Data from Bezprozvanny *et al.* (9) for $[IP_3] = 2$ μM are given by the solid marks with error bars when larger than the symbol. Predicted open probability for an IP_3-activated Ca^{2+} channel for $[IP_3] = 2$ μM (solid line) and $[IP_3] = 1.0, 0.5$, and 0.25 μM (broken lines). (*B*) Equilibrium open probability as a function of $[IP_3]$ for $[Ca^{2+}] = 0.1$ μM. The data points are from Watras *et al.* (15).

could easily be checked by using the protocols of Bezprozvanny *et al.* (9).

$[Ca^{2+}]$ Oscillations

To complete the model we add an equation that describes the $[Ca^{2+}]$ handling of the IP_3-sensitive Ca^{2+} pool,

$$\frac{d[Ca_i^{2+}]}{dt} = J_1 - J_2,$$

where $[Ca_i^{2+}]$ is the cytosolic free Ca^{2+} concentration, J_1 is the outward flux of Ca^{2+}, and J_2 is the inward flux. J_1 has two components, the Ca^{2+} flux through the IP_3 receptor/channel and a constant leak flux. Thus, the outward Ca^{2+} flux is given by

$$J_1 = c_1(v_1 x^3_{110} + v_2)([Ca^{2+}_{ER}] - [Ca_i^{2+}]),$$

where v_1 and v_2 set the maximal Ca^{2+} fluxes and $c_1 = 0.185$ is the ratio of the volume of the IP_3-sensitive Ca^{2+} pool (the ER) to the cytosolic volume (17). The inward flux, usually attributed to an ATP-dependent Ca^{2+} pump (18), is assumed to have the form,

$$J_2 = \frac{v_3[Ca_i^{2+}]^2}{[Ca_i^{2+}]^2 + k_3^2}.$$

We utilize the $[Ca^{2+}]$ conservation condition, $c_0 = c_1[Ca^{2+}_{ER}] + [Ca_i^{2+}]$, to determine $[Ca^{2+}_{ER}]$. Taking c_0 to be 2.0 μM leads to maximum values of $[Ca^{2+}_{ER}]$ and $[Ca_i^{2+}]$ of approximately 10 μM and 1.7 μM, respectively.

The remaining parameters, a_i, v_i, and k_3, were determined so that: (*i*) $[Ca^{2+}]$ oscillations occur within a reasonable range

Table 1. Standard parameters

Parameter	Value	Description
c_0	2.0 μM	Total $[Ca^{2+}]$ in terms of cytosolic vol
c_1	0.185	(ER vol)/(cytosolic vol)
v_1	6 s^{-1}	Max Ca^{2+} channel flux
v_2	0.11 s^{-1}	Ca^{2+} leak flux constant
v_3	0.9 $\mu M^{-1}\cdot s^{-1}$	Max Ca^{2+} uptake
k_3	0.1 μM	Activation constant for ATP-Ca^{2+} pump
	Receptor binding constants	
a_1	400 $\mu M^{-1}\cdot s^{-1}$	IP_3
a_2	0.2 $\mu M^{-1}\cdot s^{-1}$	Ca^{2+} (inhibition)
a_3	400 $\mu M^{-1}\cdot s^{-1}$	IP_3
a_4	0.2 $\mu M^{-1}\cdot s^{-1}$	Ca^{2+} (inhibition)
a_5	20 $\mu M^{-1}\cdot s^{-1}$	Ca^{2+} (activation)
	Receptor dissociation constants ($d_i = b_i/a_i$)	
d_1	0.13 μM	IP_3
d_2	1.049 μM	Ca^{2+} (inhibition)
d_3	943.4 nM	IP_3
d_4	144.5 nM	Ca^{2+} (inhibition)
d_5	82.34 nM	Ca^{2+} (activation)

of IP_3 (350–800 nM); (*ii*) the equilibrium $[Ca_i^{2+}]$ in the absence of IP_3 was approximately 50 nM‡; (*iii*) the qualitative nature of inhibition of Ca^{2+} release by Ca^{2+}, as experimentally found by Parker and Ivorra (12), could be reproduced (5); and (*iv*) the mean open time of the IP_3 receptor/channel is the order of a few milliseconds (15). The parameters used in the simulations, unless otherwise noted, are given in Table 1. While the parameter set given in Table 1 is not unique in satisfying the four conditions above (e.g., setting a_1 or a_5 to large values or varying certain parameters in concert gives similar results), they serve as a reference set for our numerical work.

Figs. 3 and 4 show the results of our numerical simulations. Fig. 3*A* gives the bifurcation diagram for the parameters in Table 1. Stable periodic solutions arise via Hopf bifurcations (■) and exist for 0.37 $\mu M < [IP_3] < 0.62$ μM. The periods decrease with increasing $[IP_3]$. Fig. 3*B* shows two inhibition curves that were generated by the inclusion of a simple input/decay equation for $[IP_3]$:

$$\frac{d[IP_3]}{dt} = I_r([IP_3]^* - [IP_3]) + I_p f(t), \qquad [2]$$

where $[IP_3]^*$ is the steady-state concentration, I_r is the rate constant for loss of IP_3, I_p is the pulse amplitude, and $f(t)$ (= 0 or 1) controls the timing of IP_3 pulses (5). We measure inhibition by the ratio of the height of two successive Ca^{2+} spikes resulting from equivalent IP_3 pulses. For example, an inhibition of 0.4 indicates that the second Ca^{2+} spike was 40% smaller than the first spike. The recovery time for IP_3 receptor is given by the time required for the inhibition to return to approximately 1. Fig. 4 shows two periodic solutions with fixed values of $[IP_3]$ (0.5 μM) for $a_2 = 0.2$ and $a_2 = 0.05$ $\mu M^{-1}\cdot s^{-1}$.

From our numerical simulations some generalizations can be made concerning the effect of varying certain parameters. The parameters c_0, v_1, v_3, and k_3 tend to control the $[Ca_i^{2+}]$ equilibrium level. If this level rises too high, the oscillations cease to exist. The maximum value of the IP_3 receptor/channel flux, v_1, affects the magnitude and timing of Ca^{2+} spikes; however, the Ca^{2+} spikes are limited in amplitude by the decreased open channel probability for elevated values of

‡A basal $[IP_3]$ of 240 nM was typically assumed for the numerical simulations. This gives an equilibrium $[Ca_i^{2+}]$ of approximately 95 nM.

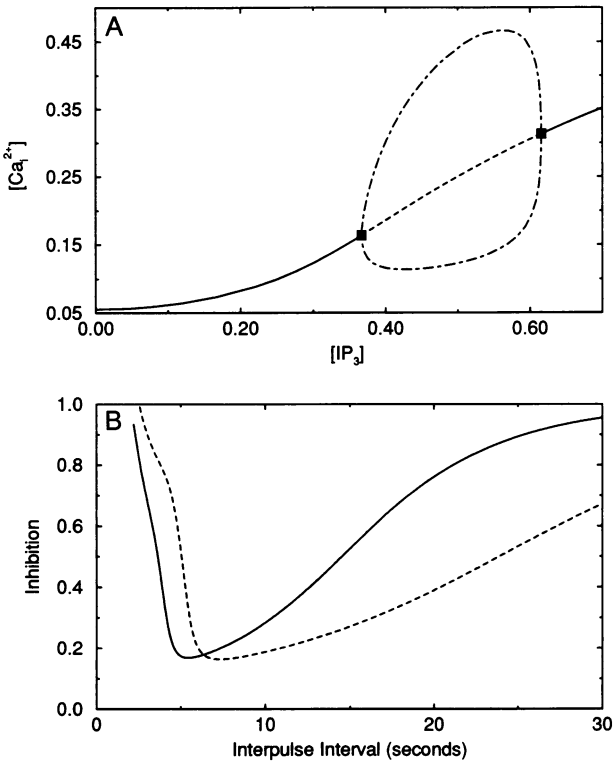

FIG. 3. (*A*) Bifurcation diagram for the reference parameters. —— indicates stable steady states, - - - indicates unstable steady states, and – – – gives the maximum and minimum cytosolic $[Ca^{2+}]$ along stable periodic orbits. Both concentrations are in μM. (*B*) Inhibition curves calculated by following the two-pulse IP_3 protocol of Parker and Ivorra (12) for the reference parameters with $[IP_3]^* = 0.24$ μM, $I_r = 1\ s^{-1}$, $I_p = 8.0$ $\mu M\cdot s^{-1}$, the length of IP_3 pulse 0.05 s, and $a_2 = 0.2$ $\mu M^{-1}\cdot s^{-1}$ (——) and $a_2 = 0.05$ $\mu M^{-1}\cdot s^{-1}$ (- - -).

$[Ca_i^{2+}]$ (cf. Fig. 2*A*). The recovery time for the IP_3 receptor/channel is affected most by a_2 and a_4 (Fig. 3*B*). Decreasing a_2 and a_4 increases the recovery time and increases the period. Generally the oscillations become more sinusoidal when the recovery time for the IP_3 receptor/channel is shorter. It is also noteworthy that the range of periods as a function of IP_3 increases as a_2 and a_4 are decreased; e.g., for $a_2 = 0.2$ $\mu M^{-1}\cdot s^{-1}$ the period ranges from 15.6 to 11.4 s, while for $a_2 = 0.05$ $\mu M^{-1}\cdot s^{-1}$ the period ranges from 25.6 to 18.5 s.

The binding kinetics of IP_3 and the activation of the receptor by Ca^{2+} are rapid (cf. Table 1), ensuring rapid release of Ca^{2+} after an IP_3 pulse. This allows the number of receptor subunit states in the model to be reduced by four. Plots of the time course of x_{0ik} vs. x_{1ik} reveal that x_{0ik} and x_{1ik} are nearly linear due to the rapid binding of IP_3. This allows us to eliminate the four receptor subunit states with IP_3 bound. Using a rapid equilibrium approximation for IP_3 binding, $x_{1ik} = ([IP_3]/d_j)x_{0ik}$ ($j = 1$ or 3), gives the following reduced system:

$$\frac{d[Ca_i^{2+}]}{dt} = J_1 - J_2, \qquad [3a]$$

$$\frac{dx_{000}}{dt} = -V_1 - V_3, \qquad [3b]$$

$$\frac{dx_{001}}{dt} = V_1 - V_4, \qquad [3c]$$

and

$$\frac{dx_{010}}{dt} = V_3 - V_2, \qquad [3d]$$

where

$$x_{ik} = ([IP_3]/d_j)x_{0ik},$$

$$V_1 = a_4([Ca_i^{2+}]x_{000} - d_4x_{001}),$$

$$V_2 = a_4([Ca_i^{2+}]x_{010} - d_4x_{011}),$$

$$V_3 = a_5([Ca_i^{2+}]x_{000} - d_5x_{010}),$$

and

$$V_4 = a_5([Ca_i^{2+}]x_{001} - d_5x_{011}),$$

with the value of x_{011} determined from the conservation condition $\Sigma_{i,j,k}x_{i,j,k} = 1$. The reduced system 3 displays the same characteristics as the full system, except that the range of $[IP_3]$ over which oscillations occur is slightly larger and, to reproduce the inhibition experiments, I_p must be lowered. This later feature is a consequence of instantaneous IP_3 binding (i.e., the channel opens more quickly at a fixed level of IP_3). The recovery time of the receptor and the period of the oscillations in the reduced model are affected most by changes in a_4, the rate constant for Ca^{2+} inhibition.

The role of Ca^{2+} in the reduced model becomes transparent when one considers the relative size of the Ca^{2+} association rate constants, a_4 and a_5. According to Fig. 1 *B* and *C*, a_5 determines the time scale for the activation by Ca^{2+} and a_4 determines the time scale for inactivation by Ca^{2+}. Because a_5 is two orders of magnitude larger than a_4, elevated $[Ca^{2+}]$ initially causes rapid activation of the IP_3 receptor/channel followed by a slow inactivation. When $[IP_3]$ is in the correct range the activation step rapidly releases Ca^{2+} into the cytosol, which ultimately inactivates the channel, leaving an opportunity for the ATPase to pump cytosolic Ca^{2+} back into the ER. When $[Ca_i^{2+}]$ has been reduced sufficiently, the inactivation disappears and the channel again rapidly activates. In this way the cycle repeats itself.

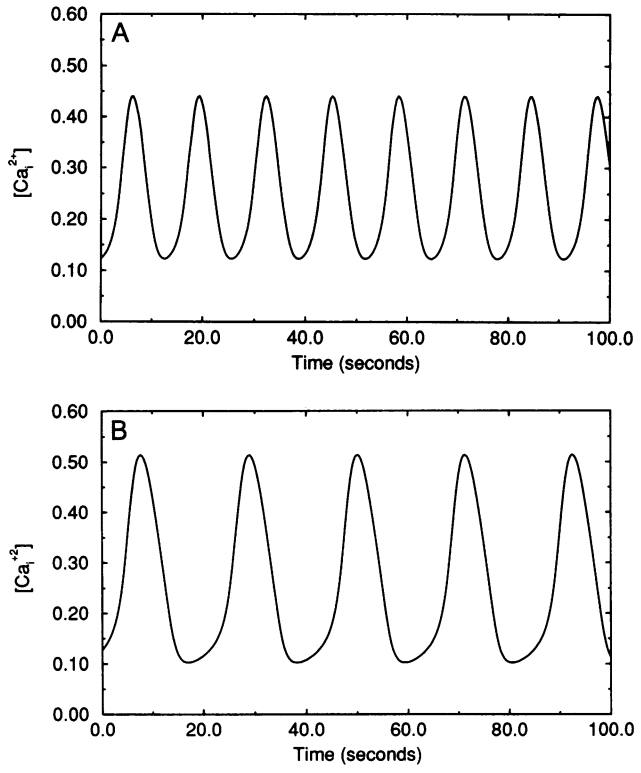

FIG. 4. Periodic orbits for the reference parameters with $[IP_3]^* = 0.5\ \mu M$ and $a_2 = 0.2\ \mu M^{-1}\cdot s^{-1}$ (*A*) or $a_2 = 0.05\ \mu M^{-1}\cdot s^{-1}$ (*B*). $[Ca_i^{2+}]$ is in μM.

Ca^{2+} Feedback on IP_3 Production

Recent experimental evidence (19–21) suggests that the production of IP_3 is dependent on $[Ca_i^{2+}]$. It is not yet known if this is caused by Ca^{2+} activation of PLC directly (19) or by an α_q subunit of a G protein (20). In either case, the $[Ca_i^{2+}]$ that produces a half-maximal IP_3 production lies within physiological ranges (0.1–3.0 μM). Although it is not yet possible to measure the degree to which IP_3 varies during oscillations, it is interesting that the present model of the IP_3 receptor/channel supports oscillation not only for constant IP_3 levels but also when significant Ca^{2+} feedback on the production of IP_3 is included.

We extend the model to include Ca^{2+} feedback on IP_3 by modifying Eq. 2 to read

$$\frac{d[IP_3]}{dt} = v_4\left(\frac{[Ca_i^{2+}] + (1-\alpha)k_4}{[Ca_i^{2+}] + k_4}\right) - I_r[IP_3], \qquad [4]$$

where $0 \le \alpha \le 1$. When $\alpha = 1$, Eq. 4 has the same sort of hyperbolic feedback that we have used to describe Ca^{2+} stimulation of IP_3 production via PLC (5). For $\alpha < 1$ Eq. 4 can be used to investigate the relative effect of Ca^{2+} stimulation of PLC on IP_3 production. Thus when $\alpha = 0$, the IP_3 production rate is v_4, which is independent of $[Ca_i^{2+}]$, while $\alpha = 0.5$ is halfway between the two extremes. The maximum rate of IP_3 production is v_4, which we assume can be increased through agonist stimulation by a G-protein mechanism. We choose k_4, the dissociation constant for Ca^{2+} stimulation of IP_3 production, to be 1.1 μM.

Fig. 5*A* shows a two-parameter continuation of the Hopf bifurcation points from $\alpha = 0$ to $\alpha = 1$ using AUTO (22). Between the broken lines the steady equilibrium solutions are unstable and stable periodic solutions exist. For nonzero α the periodic solutions are accompanied by an oscillation in $[IP_3]$. For α small the bifurcation diagram is similar to Fig. 3*A*; however, as α becomes larger both Hopf points become supercritical (Fig. 5*B*) and a stable periodic solution coexists with a stable equilibrium point. Thus the sudden appearance and disappearance of large-amplitude stable periodic solutions occurs as v_4 is slowly increased. The shape of the oscillations also changes, being characterized as sinusoidal oscillations for small α (Fig. 4*A*) and as spikes separated by long intervals of gradually increasing $[Ca_i^{2+}]$ for α near 1 (Fig. 6*A*). All stable periodic solutions increase in frequency as v_4 increases. For $\alpha = 0.8$ the periods range from 29.7 to 14.6 s. For $\alpha = 0.97$ very long orbits are possible with periods ranging from 74 to 25 s. Long-period orbits occur near the first Hopf point when it is close to the limit point (Fig. 5). One should note that the $[Ca^{2+}]$ spikes are terminated by the dynamics of the IP_3 receptor and not the exhaustion of the IP_3-sensitive Ca^{2+} pool as in two-pool models (3). The Ca^{2+} conservation condition implies a maximal $[Ca_i^{2+}]$ of approximately 1.7 μM, which implies that approximately 60% of the IP_3-sensitive Ca^{2+} pool is emptied during one spike.

Discussion

Four important qualitative conclusions can be drawn from these calculations. First, the model makes it plausible that the experimental activation and inactivation by cytoplasmic Ca^{2+} of the IP_3 receptor/channel is sufficient to produce oscillations in $[Ca_i^{2+}]$. The complete mechanism involves only a single internal pool of Ca^{2+} (the ER), which is only

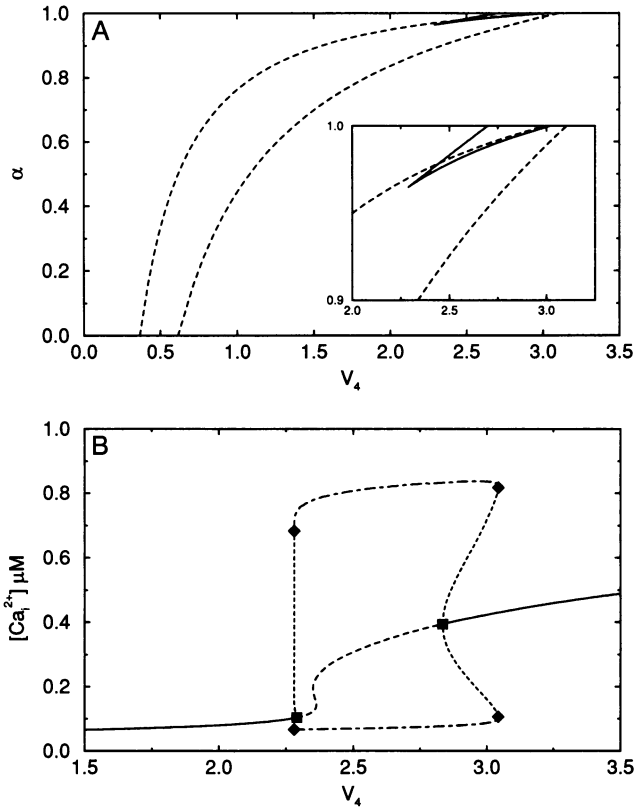

FIG. 5. (*A*) Two-parameter bifurcation diagram for the extended model. - - - indicates Hopf bifurcations and —— denotes the limit points for the equilibrium states (*Inset*). (*B*) Simple parameter bifurcation diagram for $\alpha = 0.97$. ◆ indicates a change in stability of the periodic solutions. – – – indicates the maximum and minimum of stable periodic solutions. Note the coexistence of a stable periodic solution with a stable equilibrium. v_4 is in units of s^{-1}. (All other parameters are from Table 1.)

partially emptied by a Ca^{2+} pulse and refilled through a Ca^{2+}-ATPase. We believe this to be the first model that explains oscillations on the basis of only the IP_3 receptor/channel and a single Ca^{2+} pool. Second, in this mechanism oscillations occur with the concentration of IP_3 fixed. Thus it may be relevant for experiments in which IP_3 concentrations are buffered by nonhydrolyzable IP_3 analogues (6). Third, when this mechanism is combined with positive feedback of Ca^{2+} on IP_3 production by PLC, it gives rise to sharp spikes, reminiscent of relaxation-type oscillations. Each spike is followed by a long refractory period in which Ca^{2+} concentrations are low. In this combined model, $[IP_3]$ oscillates, with its peak slightly lagging the $[Ca^{2+}]$ peak. The amplitude of the $[IP_3]$ oscillations can be as small as 0.15 μM or as large as 0.75 μM, depending on parameter values (Fig. 6). The combined mechanism may have relevance for agonist-stimulated oscillations in small cells—e.g., fibroblasts (7)—in which mixing of small molecules by diffusion to and from the plasma membrane occurs on a 0.1- to 1-s time scale, or near the plasma membrane in large cells—e.g., *Xenopus* oocytes (23, 24)—in which traveling waves of Ca^{2+} have been observed. Finally, in accord with experiments (1) we find that there are limited ranges of stimulation, either of fixed $[IP_3]$ (see Figs. 3 and 4) or agonist levels (v_4; see Fig. 6*A*), in which oscillations are possible and that the frequency increases as the level of stimulation is increased. It should be informative to explore these mechanisms in the presence of voltage-gated sources of external Ca^{2+} (25) and as models of the "excitable" cellular media responsible for Ca^{2+} waves (23).

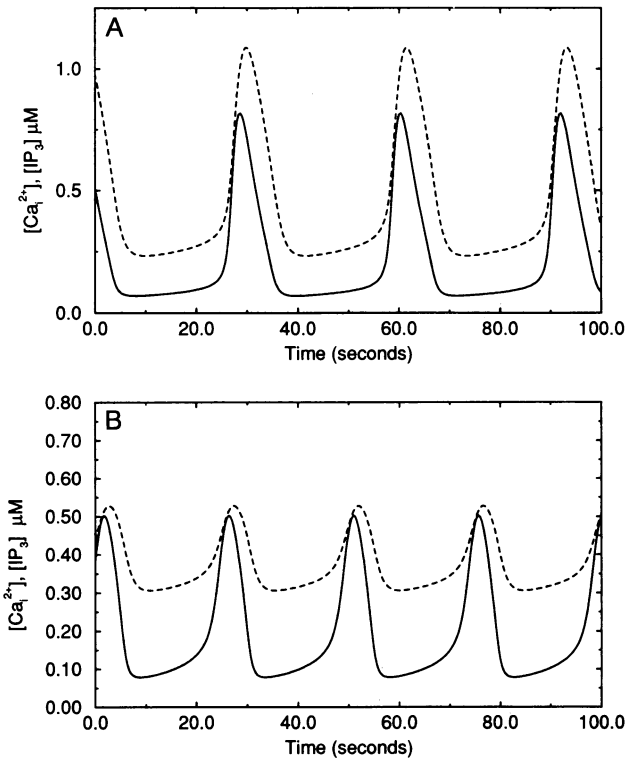

FIG. 6. Periodic solution for nonzero α. —— denotes $[Ca_i^{2+}]$; - - - denotes $[IP_3]$. (*A*) $\alpha = 0.97$ and $v_4 = 2.8\ s^{-1}$. (*B*) $\alpha = 0.8$ and $v_4 = 1.2\ s^{-1}$. (All other parameters are from Table 1.)

The authors were supported by National Science Foundation Grant DIR 90-06104 and the Agricultural Experiment Station of the University of California, Davis.

1. Berridge, M. J. (1989) in *Cell to Cell Signalling from Experiments to Theoretical Models*, ed. Goldbeter, A. (Academic, New York), pp. 449–459.
2. Meyer, T. & Stryer, L. (1991) *Annu. Rev. Biophys. Biophys. Chem.* **20**, 153–174.
3. Berridge, M. J. (1991) *Cell Calcium* **12**, 63–72.
4. Cuthbertson, K. S. R. & Chay, T. R. (1991) *Cell Calcium* **12**, 97–109.
5. Keizer, J. & De Young, G. W. (1992) *Biophys. J.* **61**, 649–660.
6. Wakui, M., Potter, B. V. L. & Petersen, O. H. (1989) *Nature (London)* **339**, 317–320.
7. Harootunian, A. T., Kao, J. P. Y., Paranjape, S. & Tsien, R. Y. (1991) *Science* **251**, 75–78.
8. Finch, E. A., Turner, T. J. & Goldin, S. M. (1991) *Science* **252**, 443–446.
9. Bezprozvanny, I., Watras, J. & Ehrlich, B. E. (1991) *Nature (London)* **351**, 751–754.
10. Yao, Y. & Parker, I. (1992) *J. Physiol. (London)*, in press.
11. Joseph, S. K., Rice, H. L. & Williamson, J. R. (1989) *Biochem. J.* **258**, 261–265.
12. Parker, I. & Ivorra, I. (1990) *Proc. Natl. Acad. Sci. USA* **87**, 260–264.
13. Ferris, C. D., Huganir, R. L., Supattapone, S. & Snyder, S. H. (1989) *Nature (London)* **342**, 87–89.
14. Meyer, T., Wensel, T. & Stryer, L. (1990) *Biochemistry* **29**, 32–37.
15. Watras, J., Bezprozvanny, I. & Ehrlich, B. E. (1991) *J. Neurosci.* **11**, 3239–3245.
16. Hill, T. (1977) *Free Energy Transduction in Biology* (Academic, New York).
17. Alberts, B., Bray, D., Lewis, J., Raff, M., Roberts, K. & Watson, J. D. (1989) *Molecular Biology of the Cell* (Garland, New York), 2nd Ed.
18. Carafoli, E. (1987) in *Annual Reviews of Biochemistry* (Annual Reviews, Palo Alto, CA), Vol. 56, pp. 395–433.
19. Mouillac, B., Balestre, M. N. & Guillon, G. (1990) *Cellular Signaling* **2**, 497–507.
20. Smrcka, A. V., Helper, J. R., Brown, K. O. & Sternweis, P. C. (1991) *Science* **251**, 804–807.
21. Taylor, S. J. & Exton, J. H. (1987) *Biochem. J.* **2488**, 791–799.
22. Doedel, E. J. & Kernevez, J. P. (1986) *AUTO: Software for Continuation and Bifurcation Problems in Ordinary Differential Equations*, Applied Mathematics Report (California Inst. of Technol., Pasadena).
23. Lechleiter, J., Girard, S., Peralta, E. & Clapham, D. (1991) *Science* **252**, 123–126.
24. Jaffe, L. F. (1991) *Proc. Natl. Acad. Sci. USA* **88**, 9883–9887.
25. Ammala, C., Larson, O., Berggren, P., Bokvist, K., Juntti-Berggren, L., Kindmark, H. & Rorsman, P. (1991) *Nature (London)* **353**, 849–852.